

12



**Abstract:** Extreme water levels, caused by the joint occurrence of storm surges and high tides, always lead to super floods along coastlines. Given the ongoing climate change, this study explored the risk of future sea-level rise on the extreme inundation by combining P-III model and losses assessment model. Taking Rongcheng as a case study, the integrated risk of extreme water levels was assessed for 2050 and 2100 under three Representative Concentration Pathways (RCP) scenarios of 2.6, 4.5, and 8.5. Results indicated that the increase in total direct losses would reach an average of 60% in 2100 as a 0.82 m sea-level rise under RCP 8.5. In addition, affected population would be increased by 4.95% to 13.87% and GDP (Gross Domestic Product) would be increased by 3.66% to 10.95% in 2050 while the augment of affected population and GDP in 2100 would be as twice as in 2050. Residential land and farmland would be under greater flooding risk in terms of the higher exposure and losses than other land-use types. Moreover, this study indicated that sea-level rise shortened the recurrence period of extreme water levels significantly and extreme events would become common. Consequently, the increase in frequency and possible losses of extreme flood events suggested that sea-level rise was very likely to exacerbate the extreme risk of coastal zone in future.

**Keywords:** sea-level rise; inundation risk; extreme water level; expected direct losses; affected population and GDP; recurrence period.

## 1 Introduction

Coastal inundation is predominantly caused by extreme water levels when storm surges are concurrent with astronomical high tides (e.g. Pugh, 2004; Quinn et al., 2014). Statistically, the extreme flood events were occurred frequently and caused huge devastation (Trenberth et al., 2015). Recent research indicated that sea-level rise, with global mean rates of 1.6 to 1.9 mm yr<sup>-1</sup> over the past 100 years (Holgate, 2007; Church and White, 2011; Ray and Douglas, 2011), had been strongly driving the floods (Winsemius et al., 2016). Global mean sea-level was expected to rise more than 1 m by the end of this century (Levermann et al., 2013; Dutton et al., 2015), even if global warming can be controlled within 2°C. Thus, coupled with continuous sea-level rise induced to climate change, the future coastal inundation risk in terms of hazards and possible losses should be paid



41 attention to disaster mitigation.

42 Projections for extreme water levels are indispensable for inundation risk assessment. Most  
 43 researches to date have focused on the coastal flooding caused by storm surges (e.g. Bhuiyan and  
 44 Dutta, 2011; Klerk et al., 2015). At present, exceedance probabilities of current extreme water level,  
 45 induced by tropical and extra-tropical storm surges, have been estimated (Haigh et al., 2014a, b).  
 46 However, on account of the sea-level rise, coastal flooding disasters would become more serious  
 47 (Feng et al., 2016) and 85% of global deltas experienced severe flooding in recent decades (Syvitski  
 48 et al., 2009). Feng and Tsimplis (2014) showed that extreme water level around the Chinese  
 49 coastline was increased by 2.0 mm to 14.1 mm yr<sup>-1</sup> from 1954 to 2012. Based on an ensemble of  
 50 projection to global inundation risk, it argued that the frequency of flooding in Southeast Asia is  
 51 likely to increase substantially (Hirabayashi et al., 2013). By 2030, the portion of global urban land  
 52 exposed to the high-frequency flooding would be increased to 40% from a 30% level in 2000  
 53 (Gunalp et al., 2015). Conservative projections suggested that over a half of global delta surface  
 54 areas would be inundated as a result of sea-level rise by 2100 (Syvitski et al., 2009).

55 The impacts of coastal flooding on social economies were considered and some methods were  
 56 established to estimate the possible losses (e.g. Yang et al., 2016). With the socio-economic  
 57 development, the large aggregations of coastal population and assets would lead to the increase  
 58 exposed to inundation in future (Mokrech et al., 2012; Strauss et al., 2012; Alfieri et al., 2015).  
 59 Without adaptation, by 2100, 0.2% to 4.6% of the global population would be at risk of flooding,  
 60 and expected annual GDP losses would be 0.3% to 9.3% (Hinkel et al., 2014). In particular,  
 61 urbanization of China was rapidly fast in the world and many low-lying coastal cities were  
 62 confronted with high probabilities of flooding (Nicholls and Cazenave, 2010). More than 30% of  
 63 the China's coast was assessed as 'high vulnerability' according the research of Yin et al., (2012),  
 64 and the population numbers exposed to flooding risk were the highest in the world (Neumann et al.,  
 65 2015). A number of China's cities including Guangzhou, Shenzhen, and Tianjin were in the top 20  
 66 global cities in terms of their exposure to 100-year inundation risk and huge average annual losses  
 67 because of water levels rising (Hallegatte et al., 2013).

68 Distinguishing the risk of extreme floods considering sea-level rise caused by climate change  
 69 is vital for disaster mitigation and adaptation on a large time scale. In this study, the flooding from  
 70 extreme water levels was simulated by a combination of storm surges, astronomical high tides, and



71 sea-level rise heights under different RCP scenarios. Using Rongcheng City as a case study, a  
72 comprehensive multi-dimensional analysis was presented to assess the inundation risk based on two  
73 time scales of 2050 and 2100, and three RCP scenarios of 2.6, 4.5, and 8.5. The main objectives are  
74 to (1) investigate the expansion of the inundated area and the increase in expected direct losses; (2)  
75 analyze the effect of sea-level rise on population and GDP; and (3) reveal the future hazard change  
76 of extreme water levels by the probability of occurrence.

## 77 **2 Data and methodology**

### 78 **2.1 Study area**

79 Rongcheng City, located at the tip of the Shandong Peninsula, China, is surrounded on three sides  
80 by 500 km of Yellow Sea coastline (Fig. 1). This city has low-elevation and flat topography and  
81 covers an area of more than 1,500 km<sup>2</sup>. Its population of 0.67 million people and GDP of \$12.31  
82 billion make it become one of the top one hundred counties in China. Rongcheng experiences a  
83 monsoonal climate at medium latitudes with an average annual rainfall of 757 mm and a temperature  
84 of 11.7°C for nearly 50 years (data from <http://data.cma.cn/>). It is also in a critical geographical  
85 position for trade exchange and the modern economy facing Korea across the Yellow Sea.  
86 Substantial additional capital investment is expected in this region because the Shandong Peninsula  
87 National High-tech Zone has been approved as a part of the National Independent Innovation  
88 Demonstration Zone by the China's State Council in 2016 (<http://www.gov.cn/>). A inundation risk  
89 assessment for Rongcheng City is urgent to its long-term development, especially under the situation  
90 of sea-level uptrend due to climate change.

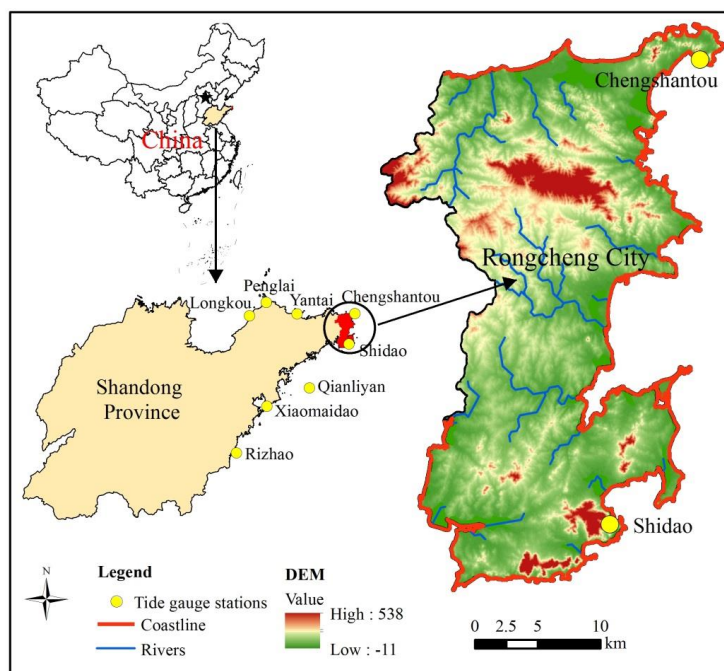


**Fig. 1** Map to show the geographic locations of Rongcheng City and main tidal gauge stations

## 2.2 Assessment process and dataset

The assessment process of inundation risk followed three steps. First, extreme water levels were calculated using storm surge data, astronomical high tides, and sea-level rise heights by the method of Pearson Type III (P-III). Second, the inundated area and depth were identified by the flood model (the four nearest neighbors algorithm) using the data of extreme water levels which resulted from the first step and the Digital Elevation Model (DEM). Third, inundation risk was assessed by direct losses model and recurrence period change. The dataset was summarized in Table 1.



107

**Table 1** Dataset of extreme risk assessment including hydrological, geographical, and statistical inputs

Data type	Content	Description	Source
Hydrological data	Sea-level rise	Global mean sea-level rise in 2050 and 2100 under RCPs 2.6, 4.5, 6.0, and 8.5. All scaled with two degrees (low vs. high)	IPCC (2013)
	Storm surge	Return periods of storm surges were obtained using the P-III model and historical data from 1967 to 2013	Tidal gauge stations, National State Oceanic Administration
	Astronomical high tide	Predicted using harmonic tide models based on measured data (Wu et al. 2016)	Tidal gauge stations, National State Oceanic Administration
Geographical data	1:10,000 digital topographic maps	A 10 m × 10 m DEM was built using elevation points and contour lines in ArcGIS	Bureau of Land Management
	Land-use maps	High precision grid data at a 30 m scale were used to characterize the land-use types in flooded area and calculate direct damage	Institute of Geographical Sciences and Natural Resources Research, Chinese Academy of Sciences (IGSNRR, CAS)
	Spatial distribution of GDP and population	1 km × 1 km grid data according to statistics from 2010	<a href="http://www.resdc.cn/">http://www.resdc.cn/</a>
Statistical data	Vulnerability curves and estimated loss values for different land-use types. Abbreviations: y, loss rate (%); x, flood depth (m); V, loss values (\$/m <sup>2</sup> ).	Residential land, $y=16.682x$ , $R^2=0.6359$ , $V=307.69$ ; Farmland, $y=49.837x$ , $R^2=0.4246$ , $V=0.77$ ; Grassland and woodland, $y=36.304x$ , $R^2=0.9113$ , $V=12.31$ ; Unused land and water regions, $y=0$ , $V=0$ .	(Yin, 2011)

108

### 109 2.3 Construction of the cumulative probability distribution of extreme water levels

110 Extreme water level is a compound event caused by storm surges and astronomical high tides while  
 111 sea-level rise also contributes to extreme water levels under global climate change. Therefore, in  
 112 this study, the current extreme water levels (CEWLs) and future extreme water levels were  
 113 constructed. The latter was a combination of CEWLs and projected heights of sea-level rise under  
 114 different RCP scenarios and was defined as the scenario extreme water levels (SEWLs). The  
 115 cumulative probability distribution curves of CEWLs and SEWLs were refitted using a P-III model  
 116 as the Equation (1). The details of this method were shown as Wu et al., (2016).



$$f(x) = \frac{\beta^\alpha}{\Gamma(\alpha)} \int_{x_p}^{\infty} (x - \alpha_0)^{\alpha-1} e^{-\beta(x-\alpha_0)} \quad (1)$$

In this expression,  $\alpha$ ,  $\beta$ , and  $\alpha_0$  are the shape, scale, and location parameters, respectively;  $x$  is the annual maximum values for water levels;  $p$  is the probability of occurrence.

$$CEWL = ST + AHT \quad (2)$$

where  $ST$  is storm surge and  $AHT$  is astronomical high tide;

$$SEWL = CEWL + SLR \quad (3)$$

where  $SLR$  is the predicted height of sea-level rise in the future;

$$T = 1/p \quad (4)$$

where  $T$  stands for the recurrence period of extreme water level and the  $T$ -year recurrence level means that an event of extreme water level has a  $1/T$  probability of occurrence in any given year (Cooley et al., 2007).

Because of the uncertain impacts of sea-level-rise on storm surges, the statistical probabilities of storm surge in this model were assumed to be unchanged in future (e.g. Hunter, 2012; Kopp et al., 2013; Little et al., 2015). The extreme water levels were mainly constructed by historical records of Chengshantou and Shidao tidal stations located in Rongcheng City (Fig. S1 in Supplementary data). In order to reduce the error caused by the spatial distribution of extreme water levels, recorded data of the surrounding six tidal stations (including Longkou, Penglai, Yantai, Qianliyan, Xiaomaidao, and Rizhao) on Shandong Peninsula were still calculated using the inverse-distance-weighted (IDW) technique in ArcGIS software.

## 2.4 Identification of flooding

Inundated area was extracted from the flood model using the four nearest neighbors algorithm based on high-resolution DEM ( $10 \text{ m} \times 10 \text{ m}$ ) and extreme water level layers ( $10 \text{ m} \times 10 \text{ m}$  cells generated in ArcGIS). Flooding criteria were that the extreme water level of layer cells must be greater than or equal to the elevation of DEM and inundated cells must be connected to the coast individually (Xu et al., 2016). The impacts of the elevations of urban landscapes and other buildings on flooding process were not considered in this study. In this section, inundated area and depth could be computed.



## 144 2.5 Inundation risk assessment

145 Expected direct losses were calculated using inundated area, inundated depth, vulnerability curves,  
 146 and loss values for each land-use type. The land-use map of 30 m resolution was resampled to 10 m  
 147 cells using the raster processing tool in ArcGIS in order to match inundated cells. The assessment  
 148 model for expected direct losses is:

$$149 \quad EDL = \sum_i A \times h \times r \times V \quad (5)$$

150 where *EDL* stands for the expected direct losses of extreme floods; *i* denotes land-use type  
 151 including residential land, farmland, woodland, grassland, and unused land; *A* denotes inundated  
 152 area; *h* stands for flood depth; *r* stands for loss rate (vulnerability curves); and *V* stands for the per-  
 153 unit loss value (\$/m<sup>2</sup>).

154 The amounts of affected population and GDP were estimated based on the grid distribution  
 155 data of population and GDP (published in China 2010 at a resolution of 1 km, <http://www.resdc.cn/>).  
 156 Land-use cover change and socio-economic development were not considered in future (Hallegatte  
 157 et al., 2013; Hinkel et al., 2014; Muis et al., 2015).

## 158 3 Results and analysis

### 159 3.1 Inundated area

160 In the absence of adaptation, the areas inundated by CEWLs and SEWLs are shown as Fig. 2. At  
 161 the present stage, inundated areas range from 156.60 km<sup>2</sup> to 168.8 km<sup>2</sup> when Rongcheng City  
 162 encounters extreme water levels. However, an expanding trend in inundated area is inevitable  
 163 because of future sea-level rise; in this analysis, the smallest increase in inundated area would be  
 164 seen under RCP 2.6 while the largest would be seen under RCP 8.5 while it would be enlarged  
 165 significantly by 2100 compared to 2050 as sea-level rise continues. The extreme scenario, under  
 166 RCP 8.5, predicts that the total area where were threatened by flooding ranges from 168.35 km<sup>2</sup> to  
 167 186.46 km<sup>2</sup> in 2050, and that it may be between 187.72 km<sup>2</sup> and 199.18 km<sup>2</sup> by 2100. According to  
 168 this projection, the maximum area is around 13% by the end of the century. At high degree for each  
 169 RCP scenario, inundated area increases by 2100 is likely to range from 14.21% to 19.54% given a  
 170 100-year recurrence. Summary statistics of future inundated area increase for 50 to 1,000-year  
 171 recurrence periods are presented in Table S1(a).



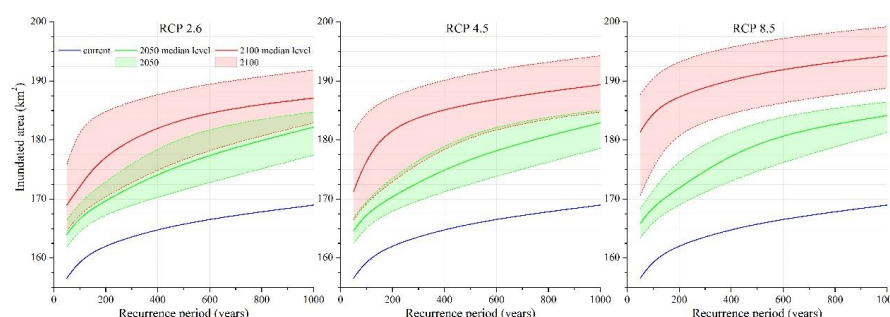


**Fig. 2** Inundated areas under different RCP scenarios for 2050 and 2100. The blue solid line denotes the inundated area curve as it changes with CEWLs, while the areas outlined by green and red stippled lines denote the extent of inundated areas projected on the basis of SEWLs under low and high degree RCP scenarios for 2050 and 2100, respectively. The green and red solid lines denote the median degree for each RCP scenario. Similarly, the explanations are used for Fig. 4 and 5.

Land-use types of residential land, farmland, woodland and grassland are involved in the estimation of total inundated area while the water bodies and unused land could be ignored in this study. Thus, summarizing the inundated data, the total inundated land-use areas under RCP 8.5 are shown in Fig. 3. Results show that residential land and farmland are more exposed to extreme water levels than woodland and grassland. Indeed, when Rongcheng City is currently subjected by extreme flooding, 42.63 km<sup>2</sup> to 46.77 km<sup>2</sup> of residential land and 34.15 km<sup>2</sup> to 39.97 km<sup>2</sup> of farmland would be affected, based on 50 to 1000-year recurrence periods, respectively. Given a high degree RCP 8.5 scenario, inundated areas of residential land and farmland would increase to 47.61 km<sup>2</sup> and 41.13 km<sup>2</sup> in 2050, and to 52.88 km<sup>2</sup> and 51.47 km<sup>2</sup> in 2100, respectively. More seriously, combined areas of residential land and farmland exposed to flooding would rise to around 50 km<sup>2</sup> in 2050 and 56 km<sup>2</sup> in 2100, respectively. The flood map (Fig. S2) shows the extension of inundated area by 2050 and 2100 given a 100-year recurrence period.

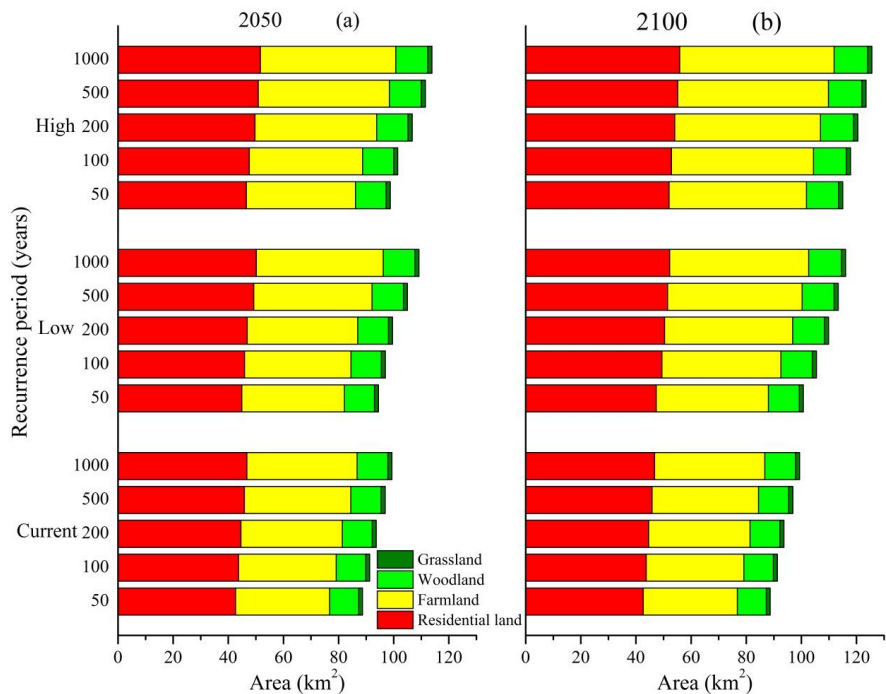


**Fig. 3** Predicted inundated areas broken down by different land-use types given 50 to 1,000-year recurrence periods in 2050 (a) and 2100 (b). RCP 8.5 is taken as an example in this paper and the inundated areas of different land-use types under RCP 2.6 and 4.5 are similar.

### 3.2 Expected direct flood losses

Flood damage does not only depend on inundated area and depth, but is related to the loss rates and values of exposed land-use types. The total expected direct flood losses would be exacerbated with sea-level rise (Fig. 4), but for current extreme floods, loss magnitudes are up to \$0.53 billion and \$0.69 billion for 50 to 1,000-year recurrence period CEWLs. Predictions for future extreme flood show an increase of more than 20% when the elevation of sea-level rise exceeds 0.3 m, however, the increase rates expand to beyond 40% given a 0.5 m sea-level rise. Indeed, by 2050, estimated losses under the RCP 2.6 scenario would be between \$0.6 billion and \$0.84 billion. These losses would be slightly increased by 2050 under the RCP 4.5 and 8.5 scenarios. Analyses show that expected direct losses would be more aggravated by the end of the century. By 2100, the smallest



range of expected damage given the low degree RCP 2.6 scenario would be between \$0.63 billion and \$0.81 billion. However, the maximum range of expected damage under the high degree RCP 8.5 scenario is predicted to be between \$0.88 billion and \$1.08 billion. It is worth noting that the increase rates reach an average of 60% under the high degree of RCP 8.5 scenario with a 0.82 m sea-level rise. The largest increase in predicted direct flood damage would be up to 29% in 2050 and 67% in 2100. Additive statistical information of future expected direct losses increase is presented in Table S1(b). The losses for main land-use types under the high degree RCP 8.5 scenario are shown in Table S2 and results indicated that residential land would be seriously affected by extreme floods.

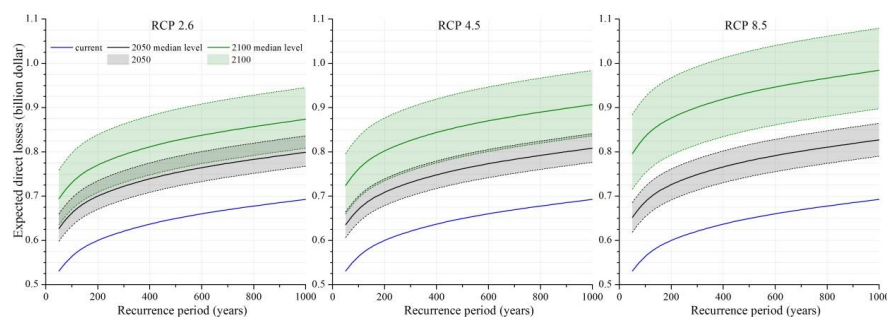


**Fig. 4** Expected direct losses (billion, dollar) in 2050 and 2100 given different RCP scenarios.

### 3.3 Population and GDP affected by extreme water levels

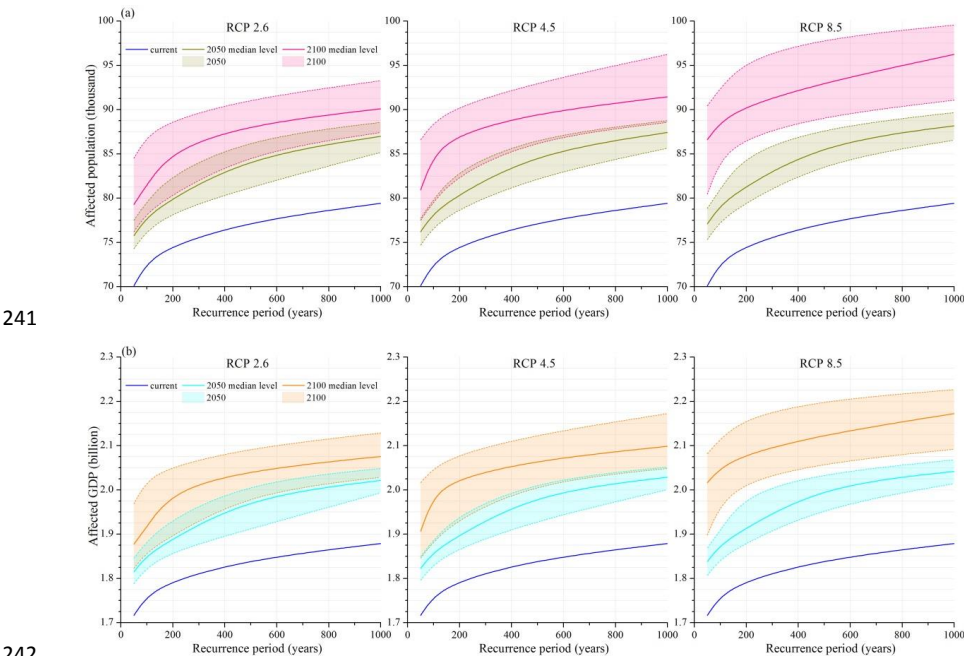
With the rapid socio-economic development, population and GDP have distributed along the coastline. Thus, a large proportion of both population and GDP are expected to be affected by extreme floods. Affected population and GDP exposed to flooding would be higher with the expansion of inundation area as a direct result of sea-level rise.

The number of affected population under RCP scenarios of 2.6, 4.5, and 8.5 is shown as Fig. 5a. Expected population magnitudes, which would suffer from 50 to 1,000-year CEWLs, range between about 70,000 and 79,000. In both 2050 and 2100, this increment is sharp with an enlarged recurrence period and the maximum increment of affected population approaches 20,000 in 2050 and 30,000 in 2100. Considering the intermediate scenario of RCP 4.5, around 5.57% to 12.36%



231 more people would be confronted with the inundation risk in 2050, while the affected population  
232 would increase 9.52% to 23.53% in 2100. Detailed data of the increase in affected population are  
233 provided in Table S1(c).

234 Similarly, sea-level rise also leads to an increased GDP exposure; the scope of affected GDP is  
235 presented in Fig. 5b. In the case of no sea-level rise, the total GDP of Rongcheng City at risk from  
236 extreme floods would be between \$1.72 billion and \$1.88 billion. As inundated area increasing due  
237 to sea-level rise, the change in affected GDP is obvious. By 2100, projections for affected GDP  
238 increase from \$1.82 billion to \$2.23 billion. At the most extreme, under the high degree RCP 8.5  
239 scenario, affected GDP would increase by approximately 20% by the end of the century. Additional  
240 information about increases in affected GDP is given in Table S1(d).



242  
243 **Fig. 5** Affected population and GDP exposed to inundation in 2050 and 2100 under different RCP scenarios

244 **3.4 Variation of recurrence periods due to sea-level rise**

245 Refitting SEWLs combined CEWLs with future sea-level rise demonstrates that the recurrence  
246 periods would decrease sharply due to climate change (Fig. 6). Results suggest that, by 2050, the  
247 recurrence periods of extreme water levels would be shortened rapidly. For example, in 2050, the  
248 100-year recurrence period for CEWL is likely to fall by eight years to 31-year (RCP 2.6), seven



years to 26-year (RCP 4.5), and five-year to 21-year (RCP 8.5). In 2100, more seriously, CEWLs would be occurred more probably becoming common events under high degree RCP scenarios. Among the different RCP scenarios, the shrink of recurrence periods under RCP 8.5 is more significant than either RCP 2.6 or 4.5 scenarios. The worst case situation is that 1,000-year recurrence period of CEWL would be occurred every three years; once in a hundred year events are likely to become common, even occurring annually by the end of this century. Such recurrence periods shortening would significantly increase the flooding risk over coming decades.

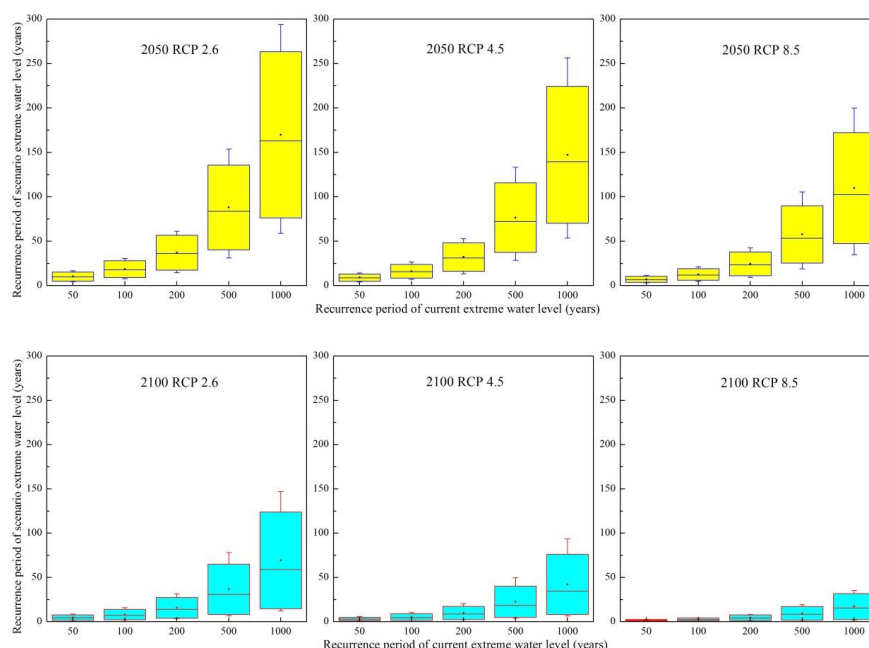


**Fig. 6** Variation in recurrence periods of CEWLs and SEWLs in 2050 and 2100 under RCP 2.6, 4.5, and 8.5

scenarios. In each RCP scenario, the variation in five representative recurrence periods of 50, 100, 200, 500 and 1000-year is shown. And the yellow boxes stand for the recurrence intervals in 2050 and the blue boxes stand for the recurrence intervals in 2100. The data, presented the variation of recurrence periods, are just referred to Chengshantou and Shidao stations.

## 4 Discussion

Based on previous studies of individual hazard and vulnerability (e.g. Li and Li, 2011; Wahl et al.,



266 2011), the extreme risk of inundation was assessed by integrating both of them. In this study, the  
 267 risk increase induced to sea-level rise was highlighted by the comparison of current with future  
 268 extreme water levels. SEWLs were recalculated by combining CEWLs with sea-level rise in 2050  
 269 and 2100 under RCP 2.6, 4.5, and 8.5. The results showed that recurrence periods would be likely  
 270 reduced by more than 70% by 2050 and this decrease could even exceed 80% by 2100 given high  
 271 RCP scenarios. In a similar study, Nicholls (2002) reported that a 0.2 m rise in sea-level could  
 272 markedly reduce recurrence periods of extreme water levels and a ten-year high water event was  
 273 converted into a six-month event. Indeed, as recurrence periods shortened, low-lying coastal areas  
 274 would have a higher probability of flood destruction over the next few decades.

275 The continuous sea-level rise would enhance the potential destructive force of future flooding.  
 276 For example, the results demonstrated that the potential inundated area would be extended by 3%  
 277 to 11% in 2050 and by 5% to 20% in 2100. In contrast, sea-level rise increased the inundated area  
 278 exposed to a cyclonic storm surge in Bangladesh by 15% with a 0.3 m rise (Karim and Mimura,  
 279 2008). Results showed that residential land and farmland were more vulnerable to sea-level rise  
 280 coupled with a large potential inundated area and a high proportion of expected direct damage.  
 281 Residential land was under the biggest risk, according to projected SEWLs under future RCP  
 282 scenarios which expected direct losses would up to \$0.6 billion in 2050 and even exceed \$1.00  
 283 billion by 2100. To put these predicted losses into context, average annual flood losses of Tianjin  
 284 City was estimated to be as high as \$2.3 billion by 2050 (Hallegatte et al., 2013). It was predicted  
 285 that Shanghai, susceptible to high water levels, would be 46% underwater by 2100 with its seawalls  
 286 and levees submerged by rising sea-levels (Wang et al., 2012). A range of studies highlighted the  
 287 fact that many coastal cities, including San Francisco, would experience flooding in the near future  
 288 as a result of rising sea-level rather than heavy rainfall (Gaines, 2016). There was no doubt that  
 289 rising sea-levels would lead to a large number of people and property would be faced with flooding  
 290 risk, especially the fast growth of China's coastal cities (McGranahan et al., 2007; Smith, 2011).

291 Given the shortening of recurrence periods in future, property and assets exposed to extreme  
 292 floods would be more likely. For instance, results showed that under a RCP 8.5 scenario, an extreme  
 293 event that was possible to take place every 1,000 years and cause damage of \$0.7 billion would  
 294 occur about once every 50 years by 2050, even once every two years by 2100. Under these  
 295 circumstances, many people and industries at extreme risk from floods would have no choice but to



296 retreat from coastal regions. However, studies indicated that most coastal populations were  
 297 completely unprepared for an increasing risk of extreme floods, especially in developing countries  
 298 (Woodruff et al., 2013).

299 Although this study manifested that sea-level rise would significantly increase the flooding risk,  
 300 some uncertainties still remain. First, on account of spatial heterogeneity, regional sea-level rise  
 301 should be projected in the future work. The objective of this paper is just to reveal the scientific  
 302 question that the impact of sea-level rise under global warming on extreme floods so that the  
 303 projection of global mean sea-level rise was used for its availability, which is consist with Wu et al.,  
 304 (2016). Nevertheless, there is no obvious land subsidence for the regional crustal stability. Second,  
 305 the combination of climate and weather extremes, including storm surges, astronomical tides,  
 306 rainfall and sea-level rise need to be focused on as they underlie and amplify the extreme events as  
 307 well as generating extreme conditions (Leonard et al., 2014). Because the coastal regions of China  
 308 have a monsoonal climate, combining inundation risk assessment with consideration of rainfall is  
 309 particularly important (Bart et al., 2015; Wahl et al., 2015). Third, human activities, which impact  
 310 on socio-economic development and alter feedbacks from climate change, are the mainly driving  
 311 force of future inundation risk (Stevens et al., 2015) and should be focused in the next research.  
 312 Consequently, the deeper exploration aiming at these uncertainties would be undertaken.

## 313 **5 Conclusions**

314 This study assessed the inundation risk resulting from extreme water levels with future projections  
 315 for 2050 and 2100 under different RCP scenarios. Results demonstrated that continuous sea-level  
 316 rise would augment the inundation risk by shortening recurrence periods and increasing the expected  
 317 losses and potential effect. (1) Sea-level rise would make low-lying coastal regions more possible  
 318 to be exposed to flood because of the recurrence periods shortening of extreme water levels. (2)  
 319 Inundation risk would be increased by the increment of inundated area, direct damage, and affected  
 320 population and GDP. (3) The analysis presented that sea-level rise principally threatened the vertical  
 321 land-use types for human survival, especially residential land and farmland. (4) Projections showed  
 322 that inundation risk would continue to increase up to 2100 and would be the most serious under the  
 323 RCP 8.5 scenario. In summary, these results revealed that sea-level rise dramatically increased the





324 flooding risk. Effective mitigation and adaptation plans are needed to deal with the increasing  
325 coastal inundation risk.

## 326 Acknowledgements

327 This research project was supported by the National Science and Technology Support Program of  
328 China (Grant No. 2013BAK05B04), the National Natural Science Foundation of China (Grant No.  
329 41301089) and the Clean Development Mechanism Funding Projects of China (Grant No. 2013034).  
330 The authors also thanked Dr. Wenhui Kuang (IGSNRR, CAS) for providing the high-precision land-  
331 use dataset of Rongcheng City.

## 332 References

- 333 Alfieri, L., Feyen, L., Dottori, F., and Bianchi, A.: Ensemble flood risk assessment in Europe under high end climate  
334 scenarios, *Glob. Environ. Chang.*, 35, 199-212, 2015.
- 335 Bart van den, H., Erik van, M., Paul de, V., Klaas-Jan van, H., and Jan, G.: Analysis of a compounding surge and  
336 precipitation event in the Netherlands, *Environ. Res. Lett.*, 10, 035001, 2015.
- 337 Bhuiyan, M. J. A. N., and Dutta, D.: Analysis of flood vulnerability and assessment of the impacts in coastal zones  
338 of Bangladesh due to potential sea-level rise, *Nat. Hazards*, 61, 729-743, 2011.
- 339 Church, J. A., and White, N. J.: Sea-Level Rise from the Late 19th to the Early 21st Century, *Surv. Geophys.*, 32,  
340 585-602, DOI 10.1007/s10712-011-9119-1, 2011.
- 341 Cooley, D., Nychka, D., and Naveau, P.: Bayesian spatial modeling of extreme precipitation return levels, *J. Am.*  
342 *Stat. Assoc.*, 102, 824-840, 2007.
- 343 Dutton, A., Carlson, A., Long, A., Milne, G., Clark, P., DeConto, R., Horton, B., Rahmstorf, S., and Raymo, M.:  
344 Sea-level rise due to polar ice-sheet mass loss during past warm periods, *Science*, 349, aaa4019, 2015.
- 345 Feng, A. Q., Gao, J. B., Wu, S. H., Liu, Y. H., He, X. J.: A review of storm surge disaster risk research and adaptation  
346 in China under climate change (In Chinese), *Progress in Geography*, 35, 1411-1419, 2016.
- 347 Feng, X., and Tsimplis, M. N.: Sea level extremes at the coasts of China, *J. Geophys. Res.*, 119, 1593-1608, 2014.
- 348 Gaines, J. M.: Flooding: Water potential, *Nature*, 531, S54-S55, 10.1038/531S54a, 2016.
- 349 Guneralp, B., Guneralp, I., and Liu, Y.: Changing global patterns of urban exposure to flood and drought hazards,  
350 *Glob. Environ. Chang.*, 31, 217-225, 2015.
- 351 Haigh, I., Wijeratne, E. M. S., MacPherson, L., Pattiaratchi, C., Mason, M., Crompton, R., and George, S.: Estimating  
352 present day extreme water level exceedance probabilities around the coastline of Australia: tides, extra-tropical  
353 storm surges and mean sea level, *Clim. Dyn.*, 42, 121-138, 10.1007/s00382-012-1652-1, 2014a.
- 354 Haigh, I. D., MacPherson, L. R., Mason, M. S., Wijeratne, E. M. S., Pattiaratchi, C. B., Crompton, R. P., and George,  
355 S.: Estimating present day extreme water level exceedance probabilities around the coastline of Australia:  
356 tropical cyclone-induced storm surges, *Clim. Dyn.*, 42, 139-157, 2014b.
- 357 Hallegatte, S., Green, C., Nicholls, R. J., and Corfee-Morlot, J.: Future flood losses in major coastal cities, *Nature*  
358 *Clim. Change*, 3, 802-806, 10.1038/nclimate1979, 2013.
- 359 Hinkel, J., Lincke, D., Vafeidis, A. T., Perrette, M., Nicholls, R. J., Tol, R. S., Marzeion, B., Fettweis, X., Ionescu,





- 360 C., and Levermann, A.: Coastal flood damage and adaptation costs under 21st century sea-level rise, *Proc. Natl.*  
361 *Acad. Sci. USA*, 111, 3292-3297, 2014.
- 362 Hirabayashi, Y., Mahendran, R., Koirala, S., Konoshima, L., Yamazaki, D., Watanabe, S., Kim, H., and Kanae, S.:  
363 Global flood risk under climate change, *Nature Clim. Change*, 3, 816-821, 2013.
- 364 Holgate, S. J.: On the decadal rates of sea level change during the twentieth century, *Geophys. Res. Lett.*, 34, Artn  
365 L01602 Doi 10.1029/2006gl028492, 2007.
- 366 Hunter, J.: A simple technique for estimating an allowance for uncertain sea-level rise, *Clim. Chang.*, 113, 239-252,  
367 2012.
- 368 IPCC: Climate Change 2013: The physical science basis: Working group I contribution to the fifth assessment report  
369 of the Intergovernmental Panel on Climate Change, Cambridge University Press, 2013.
- 370 Karim, M. F., and Mimura, N.: Impacts of climate change and sea-level rise on cyclonic storm surge floods in  
371 Bangladesh, *Glob. Environ. Chang.*, 18, 490-500, 2008.
- 372 Kirwan, M. L., and Megonigal, J. P.: Tidal wetland stability in the face of human impacts and sea-level rise, *Nature*,  
373 504, 53-60, 2013.
- 374 Klerk, W. J., Winsemius, H. C., Verseveld, W. J. v., Bakker, A. M. R., and Diermanse, F. L. M.: The co-incidence of  
375 storm surges and extreme discharges within the Rhine–Meuse Delta, *Environ. Res. Lett.*, 10, 035005, 2015.
- 376 Kopp, R. E., Simons, F. J., Mitrovica, J. X., Maloof, A. C., and Oppenheimer, M.: A probabilistic assessment of sea  
377 level variations within the last interglacial stage, *Geophys. J. Int.*, 193, 711-716, Doi 10.1093/Gji/Ggt029, 2013.
- 378 Leonard, M., Westra, S., Phatak, A., Lambert, M., van den Hurk, B., McInnes, K., Risbey, J., Schuster, S., Jakob, D.,  
379 and Stafford-Smith, M.: A compound event framework for understanding extreme impacts, *Wires Clim. Change*,  
380 5, 113-128, 10.1002/wcc.252, 2014.
- 381 Levermann, A., Clark, P. U., Marzeion, B., Milne, G. A., Pollard, D., Radic, V., and Robinson, A.: The  
382 multimillennial sea-level commitment of global warming, *Proc. Natl. Acad. Sci. USA*, 110, 13745-13750, 2013.
- 383 Li, K., and Li, G. S.: Vulnerability assessment of storm surges in the coastal area of Guangdong Province, *Nat.*  
384 *Hazards Earth Syst. Sci.*, 11, 2003-2010, 10.5194/nhess-11-2003-2011, 2011.
- 385 McGranahan, G., Balk, D., and Anderson, B.: The rising tide: assessing the risks of climate change and human  
386 settlements in low elevation coastal zones, *Environment and urbanization*, 19, 17-37, 2007.
- 387 Mokrech, M., Nicholls, R. J., and Dawson, R. J.: Scenarios of future built environment for coastal risk assessment  
388 of climate change using a GIS-based multicriteria analysis, *Environ. Plann. B*, 39, 120-136, Doi  
389 10.1068/B36077, 2012.
- 390 Muis, S., Güneralp, B., Jongman, B., Aerts, J. C. J. H., and Ward, P. J.: Flood risk and adaptation strategies under  
391 climate change and urban expansion: A probabilistic analysis using global data, *Sci. Total Environ.*, 538, 445-  
392 457, 2015.
- 393 Neumann, B., Vafeidis, A. T., Zimmermann, J., and Nicholls, R. J.: Future Coastal Population Growth and Exposure  
394 to Sea-Level Rise and Coastal Flooding - A Global Assessment, *Plos One*, 10, 10.1371/journal.pone.0118571,  
395 2015.
- 396 Nicholls, R. J.: Analysis of global impacts of sea-level rise: a case study of flooding, *Phys. Chem. Earth, Parts A/B/C*,  
397 27, 1455-1466, 2002.
- 398 Nicholls, R. J., and Cazenave, A.: Sea-Level Rise and Its Impact on Coastal Zones, *Science*, 328, 1517-1520,  
399 10.1126/science.1185782, 2010.
- 400 Pugh, D.: Changing sea levels: effects of tides, weather and climate, Cambridge University Press, 2004.
- 401 Quinn, N., Lewis, M., Wadey, M. P., and Haigh, I. D.: Assessing the temporal variability in extreme storm-tide time  
402 series for coastal flood risk assessment, *J. Geophys. Res.*, 119, 4983-4998, 10.1002/2014jc010197, 2014.
- 403 Ray, R. D., and Douglas, B. C.: Experiments in reconstructing twentieth-century sea levels, *Prog. Oceanogr.*, 91,



- 404 496-515, DOI 10.1016/j.pocean.2011.07.021, 2011.
- 405 Smith, K.: We are seven billion, *Nature Clim. Change*, 1, 331-335, 2011.
- 406 Stevens, A. J., Clarke, D., Nicholls, R. J., and Wadey, M. P.: Estimating the long-term historic evolution of exposure
- 407 to flooding of coastal populations, *Nat. Hazards Earth Syst. Sci.*, 15, 1215-1229, 10.5194/nhess-15-1215-2015,
- 408 2015.
- 409 Strauss, B. H., Ziemlinski, R., Weiss, J. L., and Overpeck, J. T.: Tidally adjusted estimates of topographic
- 410 vulnerability to sea level rise and flooding for the contiguous United States, *Environ. Res. Lett.*, 7, 014033,
- 411 2012.
- 412 Syvitski, J. P., Kettner, A. J., Overeem, I., Hutton, E. W., Hannon, M. T., Brakenridge, G. R., Day, J., Vörösmarty,
- 413 C., Saito, Y., and Giosan, L.: Sinking deltas due to human activities, *Nat. Geosci.*, 2, 681-686, 2009.
- 414 Trenberth, K. E., Fasullo, J. T., and Shepherd, T. G.: Attribution of climate extreme events, *Nature Clim. Change*, 5,
- 415 725-730, 10.1038/nclimate2657, 2015.
- 416 Wahl, T., Mudersbach, C., and Jensen, J.: Assessing the hydrodynamic boundary conditions for risk analyses in
- 417 coastal areas: a stochastic storm surge model, *Nat. Hazards Earth Syst. Sci.*, 11, 2925-2939, DOI 10.5194/nhess-
- 418 11-2925-2011, 2011.
- 419 Wahl, T., Jain, S., Bender, J., Meyers, S. D., and Luther, M. E.: Increasing risk of compound flooding from storm
- 420 surge and rainfall for major US cities, *Nature Clim. Change*, 5, 1093-1097, 2015.
- 421 Wang, J., Gao, W., Xu, S., and Yu, L.: Evaluation of the combined risk of sea level rise, land subsidence, and storm
- 422 surges on the coastal areas of Shanghai, China, *Clim. Change*, 115, 537-558, 10.1007/s10584-012-0468-7, 2012.
- 423 Winsemius, H. C., Aerts, J. C. J. H., van Beek, L. P. H., Bierkens, M. F. P., Bouwman, A., Jongman, B., Kwadijk, J.
- 424 C. J., Ligtoet, W., Lucas, P. L., van Vuuren, D. P., and Ward, P. J.: Global drivers of future river flood risk,
- 425 *Nature Clim. Change*, 6, 381-385, 2016.
- 426 Woodruff, J. D., Irish, J. L., and Camargo, S. J.: Coastal flooding by tropical cyclones and sea-level rise, *Nature*,
- 427 504, 44-52, 10.1038/nature12855, 2013.
- 428 Wu, S. H., Feng, A. Q., Gao, J. B., Li, Y. Z., Wang, L.: Shortening the recurrence periods of extreme water levels
- 429 under future sea-level rise, *Stoch. Env. Res. Risk Assess.*, 2016. doi: 10.1007/s00477-016-1327-2.
- 430 Xu, L., He, Y., Huang, W., and Cui, s.: A multi-dimensional integrated approach to assess flood risks on a coastal
- 431 city, induced by sea-level rise and storm tides, *Environ. Res. Lett.*, 11, 014001, 2016.
- 432 Yang, S., Liu, X., and Liu, Q.: A storm surge projection and disaster risk assessment model for China coastal areas,
- 433 *Nat. Hazards*, 84, 649-667, 10.1007/s11069-016-2447-1, 2016.
- 434 Yin, J.: Study on the risk assessment of typhoon storm tide in China coastal area, Shanghai: East China Normal
- 435 University, 2011.
- 436 Yin, J., Yin, Z., Wang, J., and Xu, S.: National assessment of coastal vulnerability to sea-level rise for the Chinese
- 437 coast, *J. Coast. Conserv.*, 16, 123-133, 10.1007/s11852-012-0180-9, 2012.